

Prevention of flooding in a countercurrent trickle-bed reactor using additional void space

Alex A.J. Breijer¹, John Nijenhuis, J. Ruud van Ommen^{*}

DelftChemTech, Delft University of Technology, Julianalaan 136, 2628 BL Delft, The Netherlands

Received 31 October 2006; received in revised form 19 May 2007; accepted 1 June 2007

Abstract

The influence of the configuration of additional void space (AVS) on the flooding point and the gas–liquid mass transfer coefficient ($k_L a$) of structured packings in a countercurrent trickle-bed reactor has been investigated. Experiments have been performed with six structured packings with different AVS configurations. The experiments have been performed with air, water and 3 mm glass beads in a Perspex model system. A clear difference can be observed between continuous and discontinuous AVS configurations; only continuous AVS configurations are shifting the flooding boundaries to higher gas and liquid fluxes. The $k_L a$ of all structured packings with AVS is comparable to the $k_L a$ of a cocurrent packed bed. Flooding in structured packings is qualitatively described by identifying three types of liquid flow. These flows can be manipulated with the configuration of the AVS and therefore the flooding point can be influenced. By applying AVS, flooding can also be prevented completely without loss in mass transfer ($k_L a$).

© 2007 Elsevier B.V. All rights reserved.

Keywords: Structured reactors; Packed beds; Hydrodynamics; Flow regime transition; Mass transfer; Pressure drop; Two-phase flow

1. Introduction

Cocurrent trickle-bed reactors are applied in a wide range of processes in the chemical industry, see example [1] for an extensive overview. For a number of these applications, where product inhibition occurs or the thermodynamic equilibrium is reached, countercurrent operation would be favorable. In these applications, a given conversion can be achieved with countercurrent operation with significantly less catalyst [2,3]. A major drawback of countercurrent operation is the occurrence of flooding. To prevent mass transfer limitations, usually particles of only several millimeters diameter are used. The flooding boundary of a randomly packed bed of these particles is well below the required gas and liquid fluxes for large-scale operations.

Several researchers have shown that structuring the packed bed can solve the flooding problems in a countercurrent trickle-bed. When additional void space (AVS) is added to the packed bed, the flooding boundary can be shifted to higher gas and liquid fluxes. Examples are given in literature [4–7]. Some reactive

distillation packings, such as for example the Katapak® packing manufactured by Sulzer, can also be considered as structured packed beds for countercurrent gas–liquid operation (e.g. [8]). In all of these reactors the catalyst particles are identical to the particles used in cocurrent operation. The AVS in these reactors consists of voids or channels in a randomly packed bed. The flooding boundary is shifted due to decreased drag on the gas–liquid interface, since the gas flow bypasses parts of the packed bed through the AVS.

The configuration of the AVS in the reactor designs presented in literature varies widely, but often the considerations for choosing a certain AVS configuration are not discussed. Nevertheless, the configuration of the AVS is expected to have a significant influence on the flooding boundary. The aim of this research is to gain more insight in the influence of the configuration of the AVS on the flooding boundary. Therefore, several AVS configurations are investigated, where the AVS is constructed from identical building blocks. Based on the results, a qualitative description of the phenomena that determine the flooding boundary of a countercurrent trickle-bed with AVS is proposed.

To investigate the influence of the AVS configuration on the flooding boundary, two types of structured packed beds were used. In one type the AVS is made out of wire gauze spheres. These spheres are spread throughout a randomly packed bed,

^{*} Corresponding author. Tel.: +31 15 278 2133.

E-mail address: j.r.vanommen@tudelft.nl (J.R.v. Ommen).

¹ Presently with Organon, Molenstraat 110, 5342 CC Oss, The Netherlands.

creating what could be seen as a “frozen fluidized bed”: The spheres could be considered bubbles, while the packed bed is the dense phase. In the second type of structured beds investigated in this paper the AVS is made out of wire gauze bars. The flooding boundary of three AVS configurations of each type was measured in an air–water system, with 3 mm glass beads to represent catalyst particles. As a reference, the flooding boundary of a randomly packed bed with the same glass beads was also measured.

When the gas bypasses parts of the packed bed, the gas–liquid mass transfer could decrease due to decreased contact between the gas and liquid phase. Generally, gas–liquid mass transfer is not the rate-limiting step in the processes where a countercurrent trickle-bed would be preferable, but if the mass transfer is significantly reduced this could create unwanted effects. Therefore, for a number of AVS configurations the $k_L a$ was measured and compared to literature values for the $k_L a$ of a cocurrent packed bed.

2. Experimental

The center of the experimental setup that was used is a square Perspex (polymethyl methacrylate) column with internal dimensions of 110 mm × 110 mm and a height of approximately 1 m. The bed support is made of wire gauze with a mesh of 5 mm. The 3 mm glass beads are retained by stainless steel wire gauze on top of the bed support, with a mesh of 1.8 mm and a wire thickness of 0.26 mm. The AVS elements were stacked inside the column to create the different AVS configurations, after which the glass beads are added from the top of the reactor.

In the structured packings the AVS is made from stainless steel wire gauze, with a mesh of 1.8 mm and a wire thickness of 0.26 mm. The spherical AVS elements have a diameter of 22 mm, the AVS bars are 18 mm × 18 mm × 109 mm. To ensure that the AVS elements could be fabricated in a reproducible manner, steel moulds were used to shape the wire gauze. Six different AVS configurations were built, three of each type. The six configurations are schematically shown in Fig. 1. The total porosity of all structured packings with AVS bars is 0.60; the porosities of the structured packings with AVS spheres are 0.55, 0.61 and 0.66.

Water and air were used to perform all experiments. The water enters the column through a liquid distributor with 4050 drip points per m². The height of the liquid distributor is adjustable and the liquid outlets were kept at 8 cm from the top of the bed during all experiments. Air enters the column through a tube below the bed support; a liquid level is maintained in the bottom of the reactor to prevent gas flow through the liquid exit. For more details on the experimental setup see van Hasselt et al. [6].

Flooding point measurements were performed with several structured packings and a randomly packed bed. Before every flooding point measurement with a structured packing, the bed was pre-wetted by applying a high liquid and gas flux. Visual observations confirmed that this method was effective in pre-wetting all parts of the structured packing. Pre-wetting was also attempted before the flooding measurements with a packed bed,

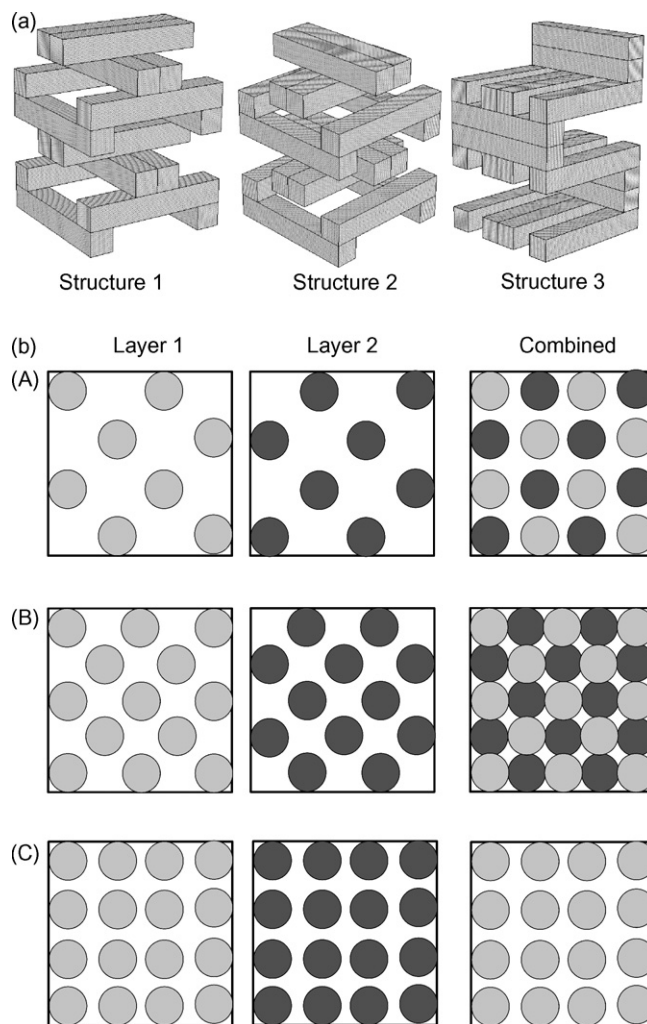


Fig. 1. (a) The three structured packings where the AVS is made from bars. Structures 1 and 3 have continuous AVS, 2 is discontinuous. Shown are the wire gauze baskets, the space in between will be filled with glass beads, which are not shown. The length and width of the structures shown are equal to the reactor dimensions. The real packings are about five times higher; (b) The AVS structures made from spheres. The different layers were stacked on top of each other. The complete packing consisted of 12–16 layers.

but flooding occurred immediately. Therefore, at the start of all flooding point measurements with a packed bed, the bed was dry or only partly wetted.

After the pre-wetting procedure, the liquid flux was set to a constant value between 1.3 and 9.7 kg m⁻² s⁻¹. The gas flux at the start of an experiment was set below 0.03 kg m⁻² s⁻¹. To measure the flooding point, the gas flow was gradually increased in steps of maximum 0.01 kg m⁻² s⁻¹. Between two changes in gas flux was a time of at least 6 min; a longer waiting period did not change the results. During the experiments the pressure drop was continuously recorded. The flooding points were determined from the average pressure drop over the last 30 s of each step in gas flux, combined with visual observations during the experiments. The flooding point was defined as the point where liquid accumulated on top of the bed and the liquid layer kept growing constantly. This is a similar definition for the flooding point as was used by Stemmet et al. [9]. To determine the flooding

point properly, a combination of the pressure drop measurements with visual observations is necessary. A sharp increase of the pressure drop is not always due to flooding, but can also be caused by accumulation of liquid on the bed support. Then the situation that arises in the bottom of the bed resembles a packed bubble-column, but no liquid accumulates on top of the bed. In literature it is reported that this effect is caused by a restrictive bed support [9].

The gas–liquid mass transfer ($k_L a$) of the structured packings where the AVS is made out of bars (structures 1–3, see Fig. 1) was measured with the oxygen absorption method at a number of liquid fluxes and gas fluxes. The dissolved oxygen concentrations at the liquid inlet and outlet were both measured with a covered membrane galvanic oxygen sensor (Cellox325, manufactured by WTW, Germany). The gas–liquid mass transfer coefficient, $k_L a$, was calculated assuming a constant gas phase composition, negligible gas-phase resistance for mass transfer, liquid plug flow and a constant temperature in the reactor. Experimental results show that less than 5% of the oxygen in the gas phase is transferred to the liquid and the Peclet numbers that were measured were typically between 30 and 50, which justifies the assumptions. With these assumptions, a molar balance for oxygen in the liquid phase gives:

$$k_L a = -\frac{1}{\tau} \ln \left[\frac{C_{O_2,liq}^* - C_{O_2,liq,out}}{C_{O_2,liq}^* - C_{O_2,liq,in}} \right] \quad (1)$$

where τ is the residence time, and $C_{O_2,liq,in}^*$, $C_{O_2,liq,out}^*$, and $C_{O_2,liq}^*$ denote the oxygen concentration in the liquid at the inlet, at the outlet, and maximum oxygen concentration in the liquid, respectively. The $k_L a$ was determined both per liquid volume and per reactor volume. To calculate the $k_L a$ per reactor volume, the liquid residence time was calculated from the liquid flux and the bed height. To determine the $k_L a$ per liquid volume, the mean liquid residence time was measured by adding short KCl pulses to the liquid feed during the experiments. The concentration in the liquid outlet was determined with a Cond340i conductivity sensor (manufactured by WTW, Germany). To correct for entrance and outlet effects, all experiments were performed with both long and short packings. The net $k_L a$ of the packing was calculated from the separate measurements by:

$$k_L a_{net} = \frac{k_L a_{long} L_{long} - k_L a_{short} L_{short}}{L_{long} - L_{short}} \quad (2)$$

where L denotes the length of the packing.

With the structured packings shown in Fig. 1, different aspects of the AVS configuration were tested. One of these aspects is whether all the AVS elements are connected, or that the gas flow is forced through parts of the packed bed. This will be referred to as continuous and discontinuous AVS, respectively. All three structured packings with AVS spheres have discontinuous AVS, one packing with bars has discontinuous AVS (structure 2). The other two AVS configurations with bars have a continuous AVS. A second aspect that is investigated in the packings with AVS bars is the variation of the amount of AVS per layer. An aspect that was tested with the AVS spheres is the distance between the spheres in the bed. This influences

the distance the gas is forced through the packed bed and the total porosity of the structured packings.

3. Results and discussion

3.1. Determination of flooding

The results of the flooding measurements for the continuous (structures 1 and 3) and the discontinuous AVS packings (structures 2 and A–C) are shown in Fig. 2a and b, respectively. As a reference, in both figures the results of the flooding measurements in a randomly packed bed are also shown. For structure 1 only two flooding points are shown in Fig. 2a, both for relatively high liquid fluxes. Several flooding experiments at liquid fluxes below $8 \text{ kg m}^{-2} \text{ s}^{-1}$ have been performed, but during none of these experiments a flooding point was measured before the maximum gas flux was reached. Also for structure 3, no flooding points were measured at liquid fluxes below $4 \text{ kg m}^{-2} \text{ s}^{-1}$, although several experiments have been performed. This result will be discussed in more detail later.

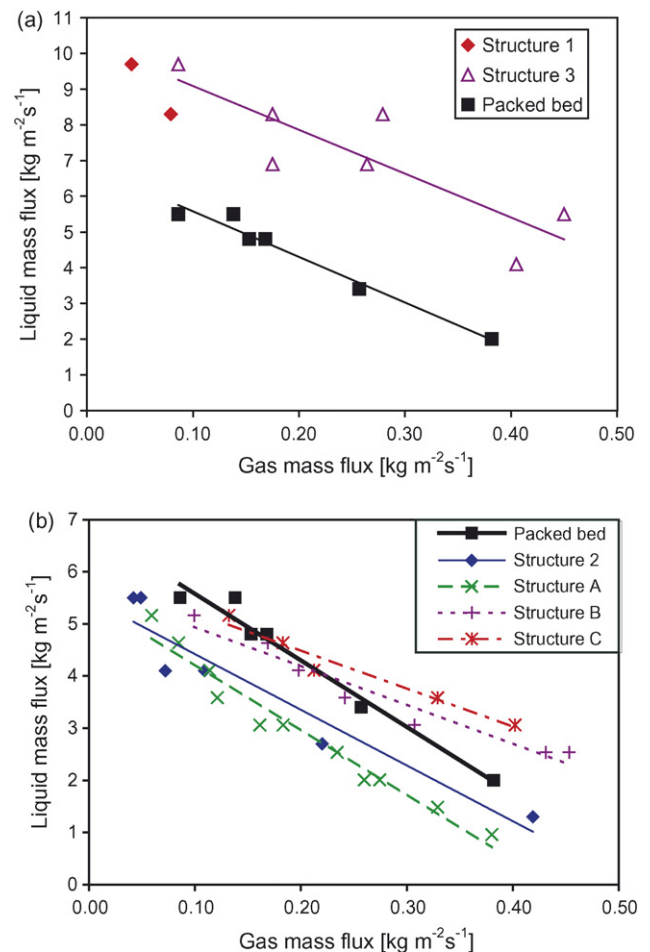


Fig. 2. (a) Results from flooding experiments with the structured packings with continuous AVS configurations. Every data point represents a measured flooding point; the lines are trend lines; (b) Flooding boundaries of structured packings with discontinuous AVS configurations. Every data point represents a measured flooding point; the lines are trend lines.

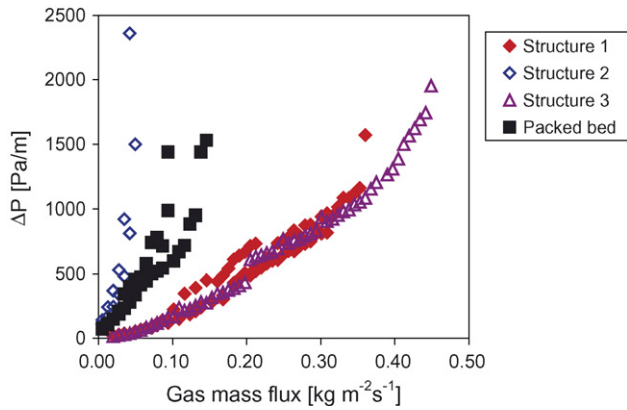


Fig. 3. Pressure drop during flooding experiments with a packed bed and the AVS configurations made out of bars at a liquid mass flux of $5.5 \text{ kg m}^{-2} \text{ s}^{-1}$.

Fig. 2a and b clearly shows that the flooding boundary of the continuous AVS configurations is much higher than the flooding boundaries of the discontinuous AVS configurations. The flooding boundaries of the discontinuous AVS configurations are close to the flooding boundary of a randomly packed bed, while the flooding boundaries of the continuous AVS configurations are significantly higher. In the two structured packings with continuous AVS, gas and liquid fluxes reported by de Wind et al. [10] for commercial hydrotreaters can be applied. However, one should keep in mind that the gas and liquid properties and the operating conditions differ from the commercial process.

The difference between continuous and discontinuous AVS can also be observed in the pressure drop characteristics. In Fig. 3 the pressure drop characteristics of the structured packings where the AVS is made from bars are compared. Although these packings have identical overall porosity, Fig. 3 shows that the pressure drop of the continuous AVS configurations is significantly lower than the pressure drop of the discontinuous AVS configuration. The pressure drop of structure 2 is of the same order of magnitude as the pressure drop of a packed bed. This same trend was observed at all other liquid mass fluxes.

Another difference that is observed between the discontinuous and continuous AVS configurations is the presence of a load point in the latter. This load point is also reported for other structured packings by Moritz and Hasse [11]. It is the point where the maximum liquid flow through the packed bed is reached, and liquid starts bypassing the packed bed. It can be observed in the pressure drop characteristic, as illustrated in Fig. 4. The load point can also be observed visually during the experiments, because at the load point a stable layer of liquid of several millimeters accumulates on top of the bed.

Surprisingly, the flooding boundary of two of the structured packings with discontinuous AVS is even lower than the flooding boundary of a packed bed (Fig. 2b). This was unexpected; it was assumed that the addition of AVS to the bed would always have a positive effect on the flooding boundary. These unexpected results can be explained with the help of observations made during the experiments. During the flooding experiments with a packed bed, it could clearly be observed that local accumulation of liquid took place inside the bed. This local liquid

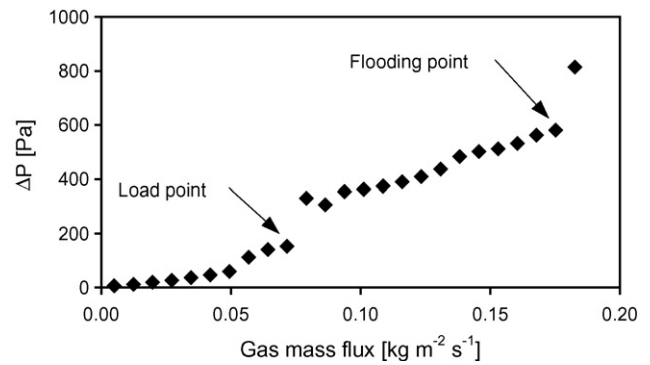


Fig. 4. A typical pressure drop characteristic, where the load point and flooding point can be observed as a sudden increase in pressure drop.

accumulation results in a layer of liquid on top of the bed of a few centimeters high. This liquid layer reaches a steady state, which means that the system does not become inoperable. When the experiment is continued, the liquid layer disappears after some time. As illustrated in Fig. 5, during flooding experiments with a packed bed this could occur several times, already at gas mass fluxes well below the flooding point. The effect was also observed several times during experiments with the structured packings.

The cause for this temporary layer of liquid on top of the packing is assumed to be non optimal liquid distribution inside the packing due to the limited size of the test reactor. It was observed during several experiments that local accumulation of liquid caused the formation of a layer of liquid in top. It is expected that in a larger reactor these small variations would not cause the accumulation of liquid, because wall effects are less significant there. Visual observations during the experiments and the results from tracer measurements did not indicate the presence of corner effects due to the square cross-section of the reactor.

During experiments with packings with discontinuous AVS, no temporary accumulation of liquid on top of the bed was observed. It is assumed that liquid also accumulates inside the packings, but instead of forming a liquid layer on top of the bed, liquid will accumulate inside the AVS. Due to their limited volume, the AVS elements will quickly be filled with liquid. The liquid accumulation blocks the gas and liquid flows and flood-

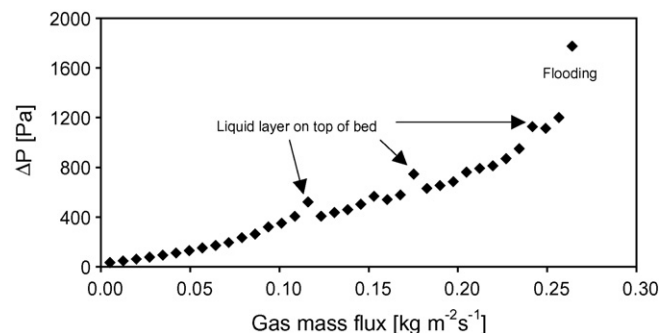


Fig. 5. Example of the accumulation of liquid on top of the bed before the flooding point is reached.

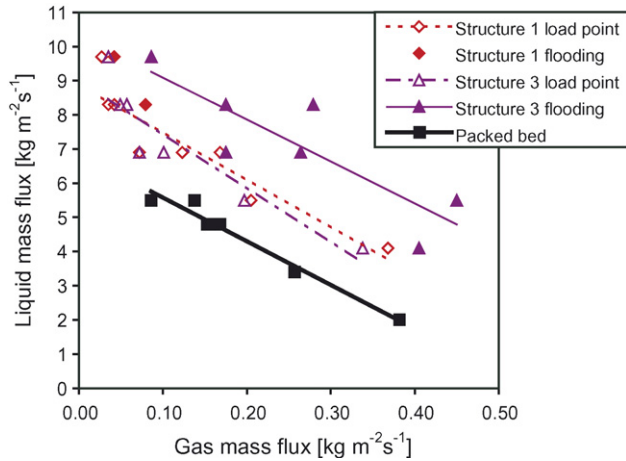


Fig. 6. Load points and flooding boundaries of structured packings with a continuous AVS configuration, compared to the flooding boundary of a packed bed.

ing will occur immediately. This could explain why the flooding boundary of some structured packings with discontinuous AVS is lower than the flooding boundary of a packed bed. In the packings with higher porosity, the distance between the AVS spheres is less and the accumulated liquid can spread through the packings more easily. This is probably the reason why the flooding boundary of structures B and C are similar to that of a packed bed.

The detailed results from the flooding experiments with the packings with continuous AVS configurations are shown in Fig. 6. Not only the flooding points are shown, but also the load points. Fig. 6 shows that at low liquid fluxes no flooding point is measured for both continuous AVS configurations. The lowest liquid flux that a flooding point was found for structure 1 was $8.3 \text{ kg m}^{-2} \text{ s}^{-1}$, for structure 3 this was $4.1 \text{ kg m}^{-2} \text{ s}^{-1}$. This means that at the maximum gas flow that could be applied ($0.50 \text{ kg m}^{-2} \text{ s}^{-1}$) still no flooding was reached. As shown in Fig. 6, for most of the lower liquid fluxes the load point was also not reached. The load points that are measured at the lower liquid fluxes are not very accurate, due to the strong influence of the pre-wetting at these conditions.

3.2. Prevention of flooding

The observation that a load and flooding point are not present below a certain liquid flux could provide a means of preventing flooding in countercurrent trickle-beds with continuous AVS. The hypothesis is that the lack of a flooding point is due to liquid that flows exclusively through the parts of the reactor with packed bed. When the liquid would only flow through the packed bed and does not enter the AVS channels, the gas flow will not influence the liquid flow and no flooding would occur. Inside the structured packings, there is the possibility for part of the liquid to flow from top to bottom exclusively through the packed bed. The cross-sectional area that is available for liquid flow exclusively through the packed bed is 44% in structure 1 and 22% in structure 3, as illustrated in Fig. 7. The maximum liquid flux that could exclusively flow through the packed bed would be the maximum liquid flux through a regular randomly packed bed, multiplied by these percentages. The calculated maximum liquid flux for structures 1 and 3 can be compared to the lowest liquid flux where a flooding point was measured, to see if they are just below them. If that is the case, it is an indication that flooding is prevented, when it is possible for the liquid to flow exclusively through the packed bed in the structured packings.

When it is assumed that the packed bed is completely filled with liquid (single phase flow), the maximum liquid flux through a packed bed can be calculated with the Ergun equation [12]. When this is done for a bed of 3 mm spherical particles, water at 20°C and gravity as the only driving force, the maximum liquid flux is $33 \text{ kg m}^{-2} \text{ s}^{-1}$. When that flux is multiplied by the percentages of the cross-sectional area that is available for flow through exclusively packed bed, the fluxes are 14.4 and $7.2 \text{ kg m}^{-2} \text{ s}^{-1}$ for configurations 1 and 3, respectively. These fluxes are much higher than the boundary values that were found in the flooding experiments.

However, it is questionable if the assumption of single-phase flow in the packed bed is valid. Visual observations during the experiments confirm that there is stagnant gas in the bed. Picaro and White [13] showed that the maximum liquid flux through a packed bed could significantly be reduced when the bed is not completely filled with liquid. Therefore, the maximum liquid

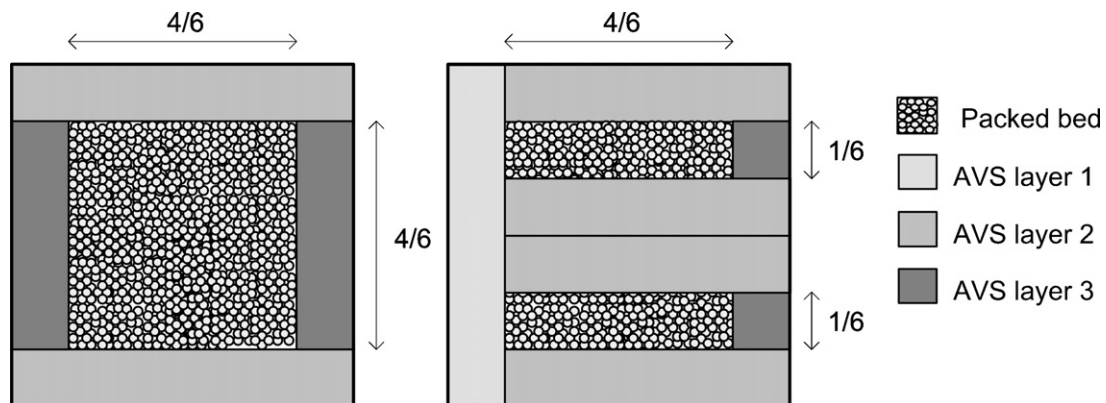


Fig. 7. Top view of parts of structures 1 (left) and 3 (right). The minimum area available for liquid flow through the packed bed is $16/36$ (44%) and $8/36$ (22%) of the total cross-sectional area, respectively.

flux through the packed bed was determined experimentally. The measured maximum flux was $15 \text{ kg m}^{-2} \text{ s}^{-1}$. When the maximum liquid flux that can flow exclusively through packed bed inside the structured packings is calculated from this result, these are 6.7 and $3.3 \text{ kg m}^{-2} \text{ s}^{-1}$ for structures 1 and 3, respectively. These fluxes are both just below the lowest liquid flux where a flooding point was found. This means that the lack of a flooding point at low liquid fluxes is because at those fluxes the liquid can flow exclusively through the packed bed. Due to the significant decrease in contact between the gas and the liquid phase, no flooding occurs.

3.3. Qualitative description of flooding in a structured packing

The aim of applying structured packings with AVS in a counter-current trickle-bed reactor is to shift the flooding boundary to higher gas and liquid fluxes. The results show a fundamental difference between continuous and discontinuous AVS configurations. Only continuous AVS configurations are successful in moving the flooding boundary to higher gas and liquid fluxes. Based on the experimental results, a qualitative description of the aspects that determine the load point and the flooding point in structured packings with continuous AVS configurations is proposed. This description is based on the assumption that there are three types of liquid flow inside structured packing with continuous AVS:

- (1) liquid flow exclusively through the packed bed. This liquid flow does not leave the packed bed while it flows down through the packing, and has little contact with the gas flow;
- (2) liquid flow alternating between the packed bed and the AVS. It flows mainly through the packed bed, but passes through the AVS channels from time to time and contacts the gas flow regularly;
- (3) liquid flow through the AVS channels. This is liquid flow bypassing parts of the packed bed through the AVS channels, thus decreasing the hydraulic diameter of these channels.

The total liquid flow is always made up of a combination of these three types. The load point and the flooding point can be qualitatively explained from the influence of the gas flow on the maximum liquid flow of each type. Every type of liquid flow is influenced by the gas flow differently. The maximum of type 1 liquid flow is independent of the gas flow and is determined by the properties of the packed bed and by the AVS configuration.

Type 2 liquid flow is influenced by the gas flow. For the liquid to pass through the AVS, it has to leave the packed bed and form droplets or jets inside the AVS. The formation of these droplets is hindered by the gas flow, which redistributes the liquid over the wire gauze. Therefore, at increasing gas flow, the maximum of type 2 liquid flow decreases.

Type 3 liquid flow decreases the hydraulic diameter of the AVS channels, and therefore further increases the gas velocity in these channels. There are two possible mechanisms that determine the maximum of type 3 liquid flow, depending on the total liquid flux. At low liquid flux, the gas velocity can reach the point

where it drags the liquid upwards and thus flooding occurs. At high total liquid flux, flooding will already have occurred before the gas velocity is high enough to drag the liquid up. At high total liquid flux, the gas flow limits the amount of liquid that can bypass the packed bed due to increased friction between the liquid and gas in the AVS channels.

The flooding point will be reached when the maximum is reached for all three types of liquid flow together and thus the total liquid flow through the reactor. This point can be reached by an increase in either gas or liquid flow. The amount of liquid fed to the top of the reactor becomes higher than the maximum liquid flow through the packing and liquid will thus accumulate inside the reactor. The load point is reached when the maximum of both types 1 and 2 liquid flow is reached. At higher liquid or gas flows, additional liquid will have to flow through the AVS channels. As mentioned before, no load point or flooding point will be reached when the total flow is lower than the maximum of the type 1 liquid flow.

The qualitative description that is proposed here could also be used to predict the load point and flooding point of structured packings. The influence of gas and liquid flow on the maximum of the three types of liquid flow can be measured separately. The data can then be combined and used to predict the load point and the flooding point. The three types of liquid flow could be manipulated individually to change the flooding boundary of the structured packing. Possibilities are for example, changes in the design of the separate AVS elements, the AVS configuration, or properties of the packed bed.

Although all experimental work was performed with water and air, the qualitative description that is proposed would also be applicable for hydrocarbon liquids and gases and for packed beds with non spherical particles. Under those circumstances, the maximum liquid flow through a packed bed would be different, but the same principle could be used to predict the flooding point.

3.4. Gas–liquid mass transfer

To investigate the influence of the configuration of the AVS on the gas–liquid mass transfer, the $k_L a$ has been measured for the three structured packings where the AVS consists of wire gauze bars (structures 1–3, see Fig. 1a). The results of these experiments are shown in Fig. 8, all corrected for entrance and outlet effects. Only the $k_L a$ values based on liquid volume ($k_{L,aL}$) are shown; the trends in the $k_L a$ per reactor volume ($k_{L,aR}$) are similar. As a reference, the $k_L a$ values for a random packed bed were also measured. These $k_{L,aL}$ values were typically 0.020 – 0.025 s^{-1} and were not significantly influenced by the liquid or gas flux. The $k_L a$ values measured for the structured packings and a random packed bed are comparable to $k_L a$ values reported for a cocurrent trickle bed reactor, for example $k_{L,aR}$ values reported by Goto and Smith [14].

The $k_L a$ experiments at every liquid flux were performed at three to four different gas fluxes, both below the load point and between the load point and flooding point. The influence of the gas flux was very small and therefore an analysis of the reproducibility of the $k_L a$ experiments was done to assess whether

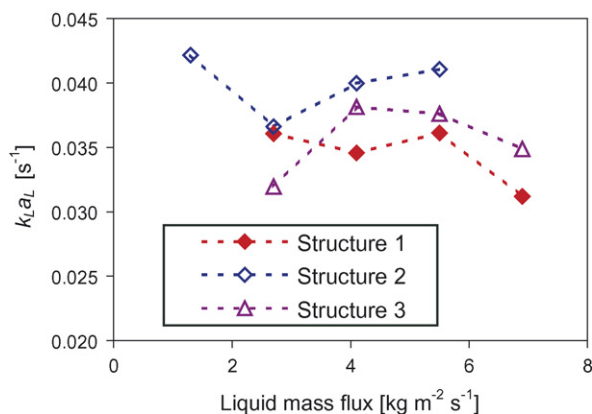


Fig. 8. Results of $k_L a$ measurements with the structured packings, based on liquid volume ($k_L a_L$). Values for different gas mass fluxes are averaged for a given liquid mass flux.

the variations are significant. The reproducibility of these $k_L a$ experiments is $\pm 15\%$, which is larger than influence of the gas flux. Therefore, in Fig. 8 results averaged over all gas fluxes per liquid flux are presented.

When the results for the $k_L a$ measurements are reviewed, no significant influence can be observed for both the liquid flux and the AVS configuration. All three structured packings consist of the same number of AVS elements and have the same porosity. From the flooding experiments, it was concluded that liquid flow through the packed bed is not influenced by the gas flow. That also implies that gas–liquid mass transfer will only take place inside the AVS channels.

All structured packings have the same porosity and also the same volume of AVS channels, which probably explains the similar $k_L a$ values. Only in structure 2, gas is forced through the packed bed that could explain the slight increase in the mass transfer. It is likely that the amount of AVS is the most important factor determining the $k_L a$. This creates possibilities to design structured packings where the $k_L a$ and the flooding boundary could be optimized separately. By changing the $k_L a$ of the AVS elements, the total $k_L a$ of the structured packing could be influenced. The shape and the dimensions of the AVS elements could be changed to achieve this.

4. Conclusions

The configuration of additional void space in a countercurrent trickle-bed reactor has a significant influence on its effectiveness in shifting the flooding boundary to higher gas and liquid fluxes. The main aspect is the difference between AVS configurations where the channels are continuous throughout the reactor, or interrupted by the packed bed. Only continuous AVS configurations are effective in significantly shifting the flooding boundary of a countercurrent trickle-bed reactor to higher gas and liquid fluxes. The flooding boundaries of discontinuous AVS configurations are similar or lower than the flooding boundary of a randomly packed bed.

A qualitative description of the liquid flows in a countercurrent trickle-bed with continuous AVS configuration is presented.

This description can be used to predict the influence of the AVS configuration on the flooding boundary. It is found that for liquid fluxes below a certain limit, no flooding point exists. This limit depends on the AVS configuration and is determined by the maximum liquid flux that can flow exclusively through packed bed without entering the AVS channels.

For a number of different AVS configurations, the gas–liquid mass transfer has been measured. There is no significant influence of the AVS configuration on the gas–liquid mass transfer in the structured packings. For every AVS configuration $k_L a$ values were measured that are comparable to a cocurrent trickle-bed reactor. It can thus be concluded, that AVS can shift the flooding boundary of a countercurrent trickle bed to significantly higher gas and liquid fluxes without a decrease in mass transfer.

The present work is meant as a first step towards a generic approach to design novel structures for counter current trickle bed reactors. Recommendations for future work include work with different structures, to generate results that further verify the qualitative description that has been proposed. To move towards industrially relevant applications, the research should also be extended to a larger scale, using gases and liquids that are used in industrial applications.

Acknowledgement

We would like to acknowledge HP Calis from stimulating discussions and Ronald van Dijk for his assistance in the experimental work.

References

- [1] M.P. Dudukovic, F. Larachi, P.L. Mills, Multiphase catalytic reactors: a perspective on current knowledge and future trends, *Cat. Rev. - Sci. Eng.* 44 (2002) 123.
- [2] J.A. Ojeda, J. Ramirez, R. Krishna, Hydrodesulphurization of gas oils: advantages of countercurrent gas–liquid contacting, in: J. Grievink, J. van Schijndel (Eds.), *European Symposium on Computer Aided Process Engineering-12*, 2002, pp. 277–282.
- [3] P. Trambouze, Countercurrent two-phase flow fixed bed catalytic reactors, *Chem. Eng. Sci.* 45 (1990) 2269–2275.
- [4] A. Kundu, S.K. Bej, K.D.P. Nigam, A novel countercurrent fixed bed reactor, *Can. J. Chem. Eng.* 81 (2003) 831–837.
- [5] H. Lin, M. Han, J. Wang, Z. Wang, Y. Jin, Study on a catalytic distillation column with a novel internal, *Chem. Eng. Commun.* 189 (2002) 1498–1516.
- [6] B.W. van Hasselt, D.J. Lindenbergh, H.P. Calis, S.T. Sie, C.M. van den Bleek, The three-levels-of-porosity reactor. A novel reactor for countercurrent trickle-flow processes, *Chem. Eng. Sci.* 52 (1997) 3901–3907.
- [7] K.D.P. Nigam, F. Larachi, Process intensification in trickle-bed reactors, *Chem. Eng. Sci.* 60 (2005) 5880–5894.
- [8] J. Ellenberger, R. Krishna, Countercurrent operation of structured catalytically packed distillation columns: pressure drop, holdup and mixing, *Chem. Eng. Sci.* 54 (1999) 1339–1345.
- [9] C.P. Stemmet, J.N. Jongmans, J. van der Schaaf, B.F.M. Kuster, J.C. Schouten, Hydrodynamics of gas–liquid countercurrent flow in solid foam packings, *Chem. Eng. Sci.* 60 (2005) 6422–6429.
- [10] M. de Wind, F.L. Plantenga, J.J.L. Heijerman, H.W. Homan Free, Upflow versus downflow testing of hydrotreating catalysts, *Appl. Catal.* 43 (1988) 239–252.

- [11] P. Moritz, H. Hasse, Fluid dynamics in reactive distillation packing Katapak-S, *Chem. Eng. Sci.* 54 (1999) 1367–1374.
- [12] S. Ergun, Fluid flow through packed columns, *Chem. Eng. Prog.* 48 (1952) 89–94.
- [13] T. Picaro, E.T. White, A preliminary study of the fluid mechanics of part-flooded beds, *Chem. Eng. Sci.* 48 (1993) 1985–1994.
- [14] Goto, Shigeo, J.M. Smith, Trickle-bed reactor performance: 1. Holdup and mass-transfer measurements, *AIChE J.* 21 (1975) 706–713.